

000 001 002 003 004 005 006 007 008 009 010 011 012 013 014 015 016 017 018 019 020 021 022 023 024 025 026 027 028 029 030 031 032 033 034 035 036 037 038 039 040 041 042 043 044 045 046 047 048 049 050 051 052 053 INSTRUCTX: TOWARDS UNIFIED VISUAL EDITING WITH MLLM GUIDANCE

Anonymous authors

Paper under double-blind review



Figure 1: Showcase of InstructX. The bottom panel presents state-of-the-art performance of InstructX in image and video editing.

ABSTRACT

With recent advances in Multimodal Large Language Models (MLLM) showing strong visual understanding and reasoning, interest is growing in using them to improve the editing performance of diffusion models. Despite rapid progress, most studies lack an in-depth analysis of MLLM design choice. Moreover, the integration of MLLM and diffusion models remains an open challenge in some difficult tasks, *e.g.*, video editing. In this paper, we present InstructX, a unified framework for image and video editing. Specifically, we conduct a comprehensive study on integrating MLLM and diffusion model for instruction-driven editing across di-

054
055
056
057
058
059
060
061

verse tasks. Building on this study, we analyze the cooperation and distinction between images and videos in unified modeling. (1) We show that training on image data can emerge video editing capabilities without explicit supervision, thereby alleviating the constraints imposed by scarce video training data. (2) By incorporating modality-specific MLLM features, our approach effectively unifies image and video editing tasks within a single model. Extensive experiments demonstrate that our method can handle a broad range of image and video editing tasks and achieve state-of-the-art performance.

062
063

064 1 INTRODUCTION

065

066 Recent research demonstrates a growing trend toward developing unified models that integrate multi-
067 modal understanding with generation. For example, systems for text-to-image generation Xie et al.
068 (2024); Zhou et al. (2024); Chen et al. (2025a), image editing Deng et al. (2025); Lin et al. (2025);
069 Liu et al. (2025); Wu et al. (2025) and video editing Liang et al. (2025); Wang et al. (2024a); Yu
070 et al. (2025), have achieved impressive results. However, how to effectively integrate Multimodal
071 Large Language Models (MLLM) with diffusion models, thereby leveraging their understanding
072 and reasoning capabilities to aid visual editing tasks, remains an open question.

073 Typical integration paradigms include: (1) autoregressive visual generation Chen et al. (2025b); Lu
074 et al. (2023); Qu et al. (2025) with discrete visual tokenizers Lee et al. (2022); Yu et al. (2021), (2)
075 hybrid AR-diffusion approaches that unify an autoregressive loss for text and a diffusion loss for
076 vision within a single transformer Zhou et al. (2024); Ma et al. (2025b); Shi et al. (2024a); Deng et al.
077 (2025), and (3) using an MLLM backbone combined with an external diffusion model as the visual
078 decoder Dong et al.; Ge et al. (2024); Sun et al. (2024); Pan et al. (2025). In this paper, we adopt
079 an external diffusion model framework because it typically converges quickly, requires minimal
080 changes, and delivers competitive performance. Although several visual editing works have been
081 developed under this paradigm Lin et al. (2025); Wu et al. (2025); Liu et al. (2025); Yu et al. (2025),
082 the role of MLLMs in the editing pipeline has yet to be examined in sufficient detail. Recently,
083 MetaQuery Pan et al. (2025) introduces a set of learnable queries that act as an interface between
084 MLLM and diffusion models. Moreover, MetaQuery employs a large connector (1.6B parameters)
085 between the MLLM and the diffusion model while keeping the MLLM parameters fixed. However,
086 a consensus has not been reached on the optimal integration of MLLM with diffusion models for
087 editing tasks. Specifically, debates persist regarding several key design choices: whether to directly
088 utilize all last hidden states or compress them into meta-query features; whether the connector should
089 be a large transformer or if a small Multi-Layer Perceptron (MLP) suffices; and whether the MLLM
090 itself requires fine-tuning. In this paper, we conduct a comprehensive study and validate a central
091 hypothesis: to fully leverage the understanding capabilities of MLLMs, they should not be treated
092 merely as feature extractors; instead, editing should be primarily realized within the MLLM, rather
093 than delegated to a subsequent large connector.

094 Collecting high-quality video data remains a bottleneck for video editing. Early works Qi et al.
095 (2023); Cong et al. (2023); Wu et al. (2023) perform video editing through zero-shot strategies, but
096 they are often limited in generation quality and generalizability. Other methods Ku et al. (2024);
097 Ouyang et al. (2024); Mou et al. (2024) transfer image editing capabilities to video by editing the
098 first frame and propagating the changes, which is prone to content drift and loss. Recently, several
099 methods Ye et al. (2025b); Zi et al. (2025b) have sought to construct video-editing datasets by training
100 video-expert models; however, these approaches suffer from lengthy data-construction pipelines
101 and low success rates. Noting that recent commercial models, such as GPT-4o OpenAI, have set
102 a new standard for instructional image editing, we leverage large-scale, high-quality image editing
103 data generated with these models to support video editing. This approach addresses both the scarcity
104 of video-editing data and the narrow range of editing types. Specifically, we train on a mixture of
105 image and video data and incorporate modality-specific MLLM features, unifying image and video
106 editing within a single model. We observe that editing capabilities learned from image data transfer
107 effectively to video editing without explicit supervision.

In summary, this paper has the following contributions:

- We present a unified framework that performs image and video editing within a single model. Our study analyzes the integration of MLLMs and diffusion models and offers insights for future research.

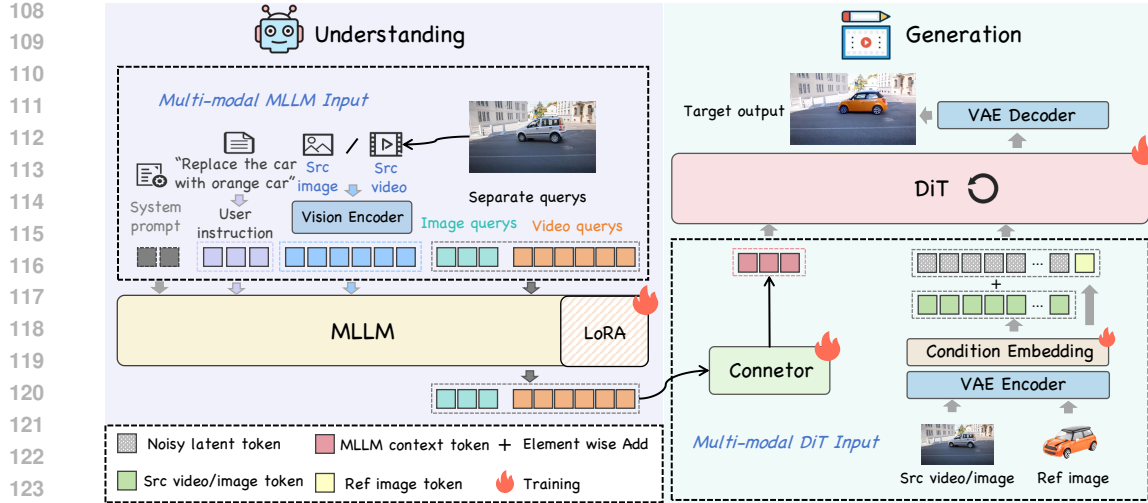


Figure 2: Overview of InstructX. The MLLM serves as the understanding module, generating editing guidance given the input instruction and visual inputs. The DiT serves as the generation module and connects to the MLLM via learnable queries and an MLP connector.

- We discuss a simple yet effective approach to extend zero-shot video editing capabilities via image training data. This design allows our method to tackle a wider range of tasks than existing open-source or closed-source methods.
- Extensive experiments show that our method achieves state-of-the-art performance across diverse image and video editing tasks.

2 RELATED WORK

2.1 INSTRUCTIONAL IMAGE AND VIDEO EDITING

Text-guided image editing significantly improves the convenience of visual manipulation by enabling users to modify images through natural language commands. Earlier approaches Nam et al. (2018); Li et al. (2020); Fu et al. (2020) primarily rely on GAN frameworks Goodfellow et al. (2020), often being constrained by limited realism and narrow domain applicability. The advent of diffusion models Ho et al. (2020) enables high-quality image editing via text. Early works learn from synthetic input-goal-instruction triples Brooks et al. (2023) and with additional human feedback Zhang et al. (2024b) to follow editing instructions. Fu et al. (2023) investigates how MLLM facilitate edit instructions. Recently, as MLLM grows in scale and demonstrates stronger capabilities in instruction understanding, several unified modeling approaches Lin et al. (2025); Liu et al. (2025); OpenAI; Zeng et al. (2025) are proposed, improving the performance of image editing. When it comes to video editing, the challenge becomes significantly harder. Limited by model capabilities and training data, early research Qi et al. (2023); Cong et al. (2023); Wu et al. (2023) primarily relies on zero-shot or one-shot approaches based on image diffusion models. Later, with the performance scale-up of video diffusion models, several downstream tasks emerge, leveraging pre-trained video diffusion models. Examples include video inpainting Zi et al. (2025c); Bian et al. (2025), video try-on Fang et al. (2024); Zuo et al. (2025), and video addition Tu et al. (2025); Zhuang et al. (2025). Recently, some unified modeling methods Liang et al. (2025); Yu et al. (2025); Ye et al. (2025b) are proposed for video editing. However, these methods are constrained by manual priors, such as specifying editing areas and motion trajectories. Instruction-based editing offers a more convenient way. Early research, InsV2V Cheng et al. (2023), adapt image instruction editing model Brooks et al. (2023) to generate video training pairs. However, due to limitations in data quality, the editing results are often unsatisfactory. Very recent studies Tan et al. (2025) integrate the comprehension capabilities of MLLM into video editing. However, model designs are often not justified experimentally or very briefly, and the scope of tasks remains limited by the training data.

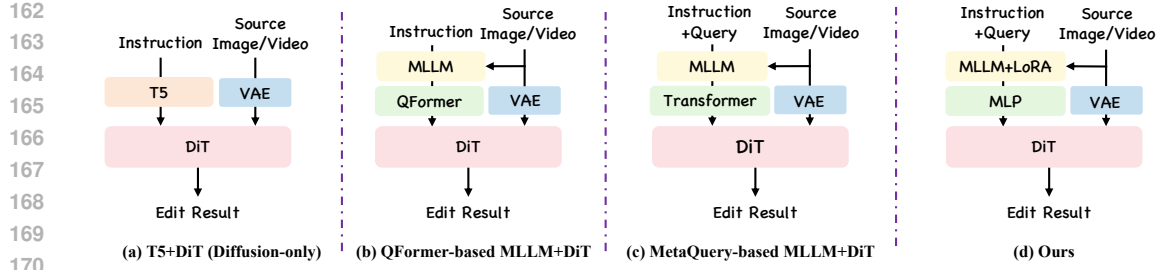


Figure 3: Different design choices for unified editing modeling.

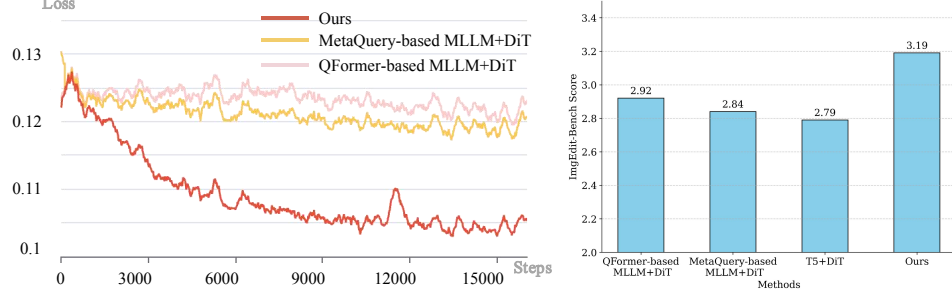


Figure 4: Illustration of alignment ability (left) and editing performance (right) for different design choices.

2.2 UNIFIED UNDERSTANDING AND GENERATION MODELS

Recently, extensive attempts extend the success of multimodal understanding to multimodal generation. Some works learn to regress image features Ge et al. (2024); Sun et al. (2023); Tong et al. (2024); some works auto-regressively predict the next visual tokens Jin et al. (2023); Team (2024); Xie et al. (2024); and some works Zhou et al. (2024); Ma et al. (2025b); Shi et al. (2024a); Deng et al. (2025) employ diffusion objective for visual generation and autoregressive objective for text generation. In this field, using a connector Dong et al.; Ge et al. (2024); Sun et al. (2024) to bridge the understanding model and diffusion model is a strategy for rapid convergence, while also delivering promising results. Recent work on MetaQuery Pan et al. (2025) introduces a useful bridging method through a set of learnable queries. However, for visual editing, several questions arise: whether to use all final hidden states directly or compress them into meta-queries; whether a large connector is necessary; and whether freezing the MLLM is sufficient. We study these questions in this work.

3 METHOD

3.1 OVERVIEW

An overview of InstructX is presented in Fig. 2. Recall that our goal is to build a unified architecture for image and video editing by leveraging the comprehension capabilities of MLLM. To this end, we employ a multimodal understanding model, *i.e.*, QWen2.5-VL-3B Bai et al. (2025), to embed the editing instruction and source image/video. Inspired by MetaQuery Pan et al. (2025), we append a set of learnable queries to the MLLM input sequence to extract editing information and retain only the meta-query features from the MLLM output. Wan2.1-14B Wan et al. (2025) is used as the decoder for the edited output. The produced queries from the MLLM are fed into a two-layer MLP connector, and are subsequently used to replace the text embeddings in the DiT model. To enhance the consistency between the edited result and the source image/video, we add the VAE encoding of the original image/video to the noisy latent. For tasks involving a reference image, we concatenate the VAE features of the reference image to the noisy latent along the sequence dimension.

3.2 ARCHITECTURE CHOICE

Different choices. As noted above, integrating understanding and generation models exposes many design choices that are often not empirically justified in prior work. We conduct a comprehensive study of these structural design choices. In Fig. 3, we compare several instruction-editing architec-

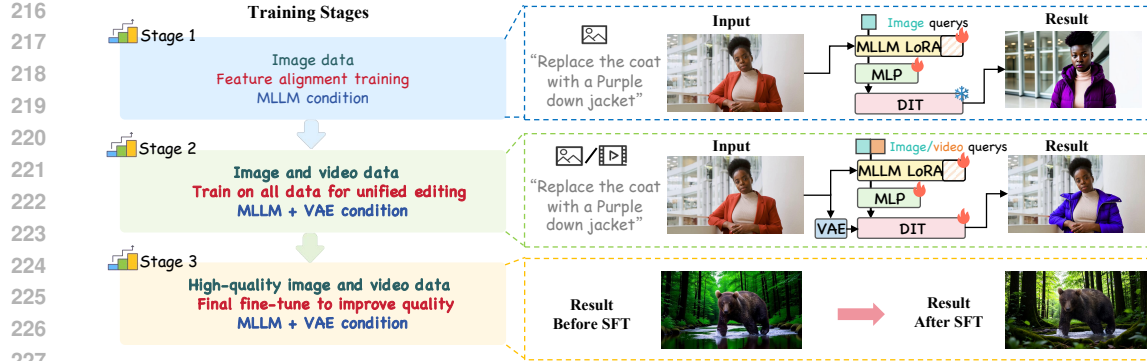


Figure 5: Illustration of three training stages of our methods.



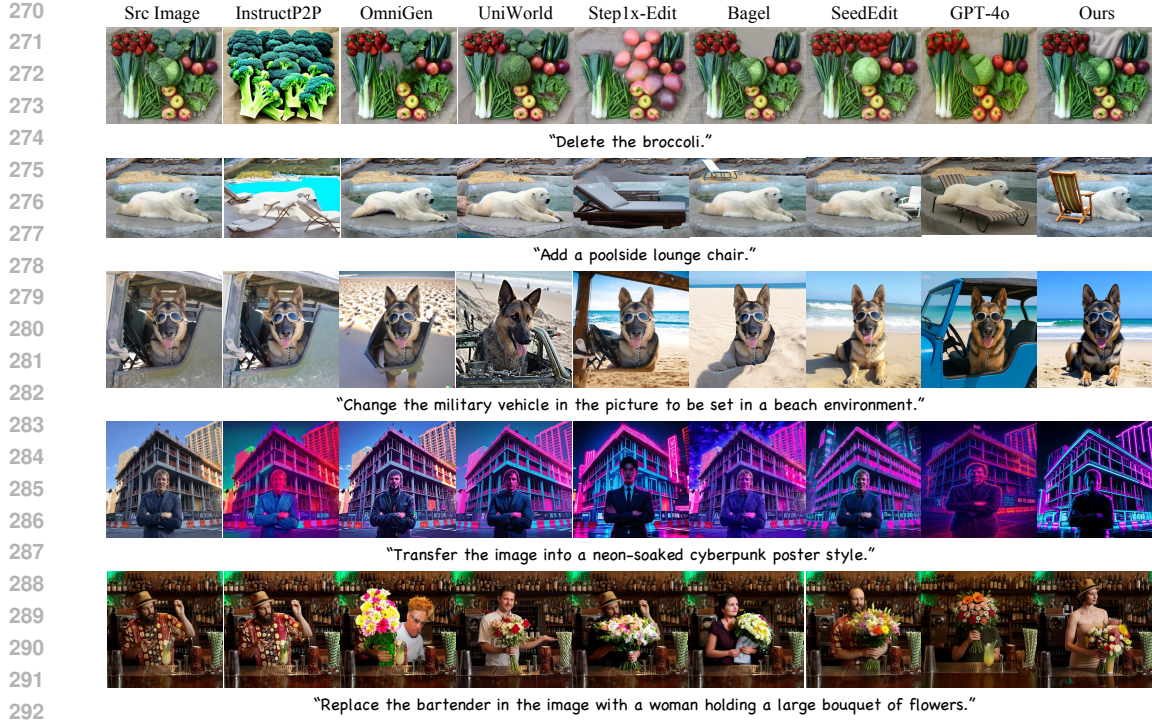
Figure 6: Examples for emergent video editing capabilities through image data.

tures: (a) Instructions are encoded by the native T5 text encoder Chung et al. (2024) and fed directly into the diffusion model, *i.e.*, diffusion-only setting. (b) The last hidden states of the MLLM are encoded by QFormer Li et al. (2023) into fixed-length representation (*i.e.*, 256 tokens), which is then input to DiT. (c) The MetaQuery Pan et al. (2025) structure uses learnable queries to extract editing information from the MLLM and employs a large connector to bridge the MLLM and the DiT. (d) The architecture adopted in this work. It uses the same learnable queries as MetaQuery, fine-tunes the MLLM LoRA, and employs a simple two-layer MLP as the connector between MLLM and DiT.

Comparsion. We validate the performance of different structure choices from two aspects. (1) Feature alignment capability. Due to the gap between the MLLM text space and the diffusion generation space, previous works Dong et al.; Ge et al. (2024) usually incorporate a pre-training stage to align these two spaces. Here, we freeze the DiT and train different designs on image editing task. The left part of Fig 4 shows that solely relying on a large-scale connector or a learnable query mechanism for the understanding-generation alignment converges slowly. Partially involving MLLM in feature alignment via LoRA Hu et al. (2022) accelerates convergence. Note that the T5 features are already aligned with DiT, hence not involved in this stage. Upon completion of the alignment stage, we unfreeze the DiT for continued training and evaluate the performance of various methods on ImgEdit-Bench Ye et al. (2025a). The right part in Fig. 4 also shows an advantage of the design choice in this paper. We also provide a further discussion on the gains of MLLM in the appendix A.8. **Other details.** Moreover, to model images and videos in a unified architecture while distinguishing between the two modalities, we introduce separate sets of learnable queries for each: 256 queries for image inputs and 512 queries for video inputs. Note that for video input, we specifically sample 13 frames to serve as input to the MLLM. Further experimental details are provided in Sec. 4.4.

3.3 TRAINING STRATEGIES

Three stages. As shown in Fig. 5, the training process is divided into three stages: feature alignment training, full-data training, and quality fine-tuning. **Stage 1:** The target of the first stage is to align the feature space of the MLLM with the generation space of the DiT. During this stage, we only train the learnable query, the LoRA in the MLLM, and the MLP connector on the image-instruction data. After this stage, the model acquires a rough instruction-based editing capability. However, due to the coarse-grained visual information in the MLLM, the editing results exhibit poor consistency with the original image. **Stage 2:** The second stage has two objectives: (1) Improving the fidelity between



324 from the video data but present in the image data. After mixed training, the model also acquires
 325 the capability for video style transfer. **Stage 3:** Although the model acquires unified image/video
 326 editing capabilities after the second stage, the generation quality is affected by some low-quality
 327 training data, resulting in the oily and plastic-like textures. To rectify this problem, we collect a
 328 small amount of high-quality training data and perform quality fine-tuning. As shown in the last
 329 row of Fig. 5, the generated results become more natural and aesthetically pleasing after quality
 330 fine-tuning. We use flow-matching Lipman et al. (2022) as the training objective in all stages.

331 **Training data.** For instruction-based image editing, we utilize large-scale open-source training
 332 data, including NHR-Edit Kuprashevich et al. (2025), X2Edit Ma et al. (2025a), and GPT-Image-
 333 Edit Wang et al. (2025b). For video editing, due to the lack of high-quality open-source video
 334 editing data, we develop a pipeline for synthesizing video-editing data. More details are provided in
 335 the appendix A.2.

336 4 EXPERIMENT

337 4.1 IMPLEMENTATION DETAILS

339 During training, we set the learning rate to 1×10^{-5} , with a global batch size of 128 for images
 340 and 32 for videos. In the first and second training stages, we iterate for 20,000 steps each, while the
 341 third stage involves 5,000 iterations. During the image/video mixed training, we sample video data
 342 with a probability of 0.6 and image data with a probability of 0.4.

343 4.2 EVALUATION DETAILS

345 For image editing, we compare different methods on two benchmarks: ImgEdit-Bench Ye et al.
 346 (2025a) and GEdit-Bench Liu et al. (2025). Specifically, on ImgEdit-Bench, we use GPT-4.1 Ope-
 347 nAI to score the editing results on a 1-5 scale. On GEdit-Bench, we employ Qwen2.5-VL-72B Bai
 348 et al. (2025) to evaluate the edited results across three metrics: instruction-following score (Q_SC),
 349 perceptual-quality score (Q_PQ), and overall score (Q_O). We compare our method with the well-
 350 known instruction-based image editing method (*i.e.*, InstructPix2Pix Brooks et al. (2023)), recent
 351 state-of-the-art approaches (*i.e.*, OmniGen Xiao et al. (2025), Uniworld Lin et al. (2025), Step1x-
 352 Edit Liu et al. (2025), Bagel Deng et al. (2025)), as well as several closed-source models (GPT-
 353 4o OpenAI, DouBao Shi et al. (2024b)).

354 For video editing, existing benchmarks(*e.g.*, UNICBench Ye et al. (2025b) and VACE-
 355 Benchmark Jiang et al. (2025)) primarily focus on target-prompt rather than instruction-prompt eval-
 356 uation and provide few examples per task. To address the lack of instruction-based video-editing
 357 benchmarks, we introduce VIE-Bench, which comprises 140 high-quality instances across eight
 358 categories, covering both reference-free and reference-based edits. Further details are provided in
 359 Appendix Sec. A.1. Prior work commonly uses the CLIP text score to assess text-video alignment,
 360 which is effective for target-prompt settings but fails to capture instruction-following capability.

361 Therefore, we adopt an MLLM-based
 362 judge using GPT-4o OpenAI to evaluate
 363 editing accuracy (instruction following),
 364 preservation (consistency with
 365 the source video), and quality (overall
 366 video quality). For reference-based

367 editing, GPT-4o also assesses subject
 368 similarity to the reference image. All
 369 scores range from 1 to 10. The system
 370 prompts for the MLLM-based judge
 371 are provided in Appendix Sec. A.9. In
 372 addition, we employ VBench Zhang
 373 et al. (2024a) to evaluate video qual-
 374 ity. We compare our method with the
 375 well-known baseline InsV2V Cheng
 376 et al. (2023), recent state-of-the-art
 377 approaches (VACE-14B Jiang et al. (2025),
 378 Omni-Video Tan et al. (2025)), and
 379 closed-source systems (Kling Keling
 380 (2025), Pika Pika (2025), Runway-Aleph Runway (2025)). For the removal task, we also evaluate
 381 against MiniMax-Remover Zi et al. (2025a) and DiffuEraser Li et al. (2025).

382 Table 1: **Comparison results on GEdit-Bench.**
 383 Q_SC, Q_PQ, and Q_O refer to the metrics evaluated
 384 by Qwen-2.5-VL-72B. The best and second best results
 385 are shown in **bold** and underlined respectively.

Model	Community Model	Q_SC↑	Q_PQ↑	Q_O↑
Ours	✓	7.47	<u>7.22</u>	6.68
Step1X-Edit	✓	7.05	7.21	<u>6.79</u>
Instruct-P2P	✓	5.08	6.86	4.90
OmniGen	✓	6.33	6.96	6.04
UniWorld	✓	5.43	7.37	5.35
Bagel	✓	<u>7.43</u>	7.03	7.10
SeedEdit 3.0	✗	7.92	7.39	7.57
GPT-4o	✗	<u>7.98</u>	7.73	7.83

378
 379 Table 2: **Comparison results on ImgEdit-Bench.** “Overall” is calculated by averaging all scores
 380 across tasks. We use Qwen2.5-VL-72B for evaluation. The best and second best results are shown
 381 in **bold** and underlined respectively.

382 Model	383 Community Model	384 Adjust	385 Remove	386 Replace	387 Add	388 Style	389 Compose	390 Background	391 Action	392 Overall↑
384 Ours	✓	3.56	3.92	4.03	3.7	<u>4.45</u>	3.27	<u>3.63</u>	4.24	3.85
Step1X-Edit	✓	3.27	3.13	<u>3.91</u>	2.75	4.53	2.38	3.67	3.48	3.39
Instruct-P2P	✓	2.53	1.11	1.50	1.89	3.44	1.61	1.65	2.35	2.01
OmniGen	✓	2.04	2.09	2.02	3.33	3.65	3.58	2.46	1.97	2.64
UniWorld	✓	2.95	<u>3.54</u>	2.64	4.04	3.33	2.91	3.07	2.55	3.13
BAGEL	✓	<u>3.51</u>	3.27	3.26	<u>3.81</u>	4.26	3.11	2.62	4.31	3.52
SeedEdit 3.0	✗	2.43	4.27	4.33	4.40	4.51	4.32	3.58	4.62	4.06
GPT-4o	✗	4.15	4.54	4.49	4.84	4.63	4.30	4.87	4.22	4.51

392
 393 Table 3: **Comparison results on VIE-Bench.** The best and second best results are shown in **bold**
 394 and underlined respectively.

395 Task	396 Method			397 VIE-Bench Score					398 Video Quality	
	399 Model	400 Community Model	401 Instruction base	402 Instruct-follow	403 Preservation	404 Quality	405 Similarity	406 Avg.	407 Smoothness	408 Aesthetics
399 Video Edit										
400 Add	401 Ours	✓	✓	8.446	<u>8.683</u>	7.919	-	8.349	0.991	0.558
	Kling	✗	✓	6.000	8.230	5.576	-	6.602	0.988	0.519
	Runway	✗	✓	8.607	8.913	<u>7.823</u>	-	8.447	<u>0.990</u>	0.557
	Omni-Video	✓	✓	5.699	6.135	6.294	-	6.242	0.987	0.586
	InsV2V	✓	✓	3.552	5.891	3.402	-	4.281	0.988	0.513
	VACE	✓	✗	3.938	6.696	3.929	-	4.854	0.983	0.557
404 Swap / Change	405 Ours	✓	✓	<u>9.514</u>	9.171	<u>8.533</u>	-	9.072	0.977	0.557
	Kling	✗	✓	9.000	<u>9.060</u>	8.333	-	8.800	0.989	0.541
	Runway	✗	✓	9.580	8.628	9.275	-	9.161	<u>0.981</u>	0.541
	Pika	✗	✓	7.542	7.847	6.837	-	7.408	0.974	0.528
	Omni-Video	✓	✓	4.733	4.856	4.656	-	4.748	<u>0.981</u>	<u>0.556</u>
	InsV2V	✓	✓	5.304	6.428	4.971	-	5.567	0.977	0.530
410 Remove	411 Ours	✓	✓	8.627	8.668	<u>7.672</u>	-	8.322	0.983	0.472
	Kling	✗	✓	8.440	<u>8.800</u>	7.520	-	8.253	0.993	0.455
	Runway	✗	✓	8.664	9.145	<u>7.703</u>	-	8.504	0.987	0.460
	Omni-Video	✓	✓	6.004	5.970	4.807	-	5.593	0.989	0.417
	InsV2V	✓	✓	1.209	3.769	1.322	-	2.098	0.982	<u>0.517</u>
	VACE	✓	✗	1.812	3.877	2.359	-	2.682	0.983	0.535
414 Style / Tone Change	415 Ours	✓	✓	6.963	7.518	6.037	-	6.839	0.985	0.467
	MiniMax	✓	✗	6.935	7.552	6.199	-	6.640	0.976	0.534
	DiffuEraser	✓	✗	6.346	6.807	5.576	-	6.243	0.986	0.465
	Runway	✗	✓	9.650	<u>9.099</u>	8.839	-	9.196	0.972	0.560
418 Hybrid Edit	Omni-Video	✓	✓	<u>9.583</u>	9.200	<u>8.616</u>	-	9.133	0.982	0.547
	InsV2V	✓	✓	5.486	4.655	5.959	-	5.366	0.984	<u>0.557</u>
	Ours	✓	✓	7.835	8.086	6.437	-	7.452	0.971	0.529
	Runway	✗	✓	9.448	8.862	<u>8.411</u>	-	8.907	0.973	<u>0.590</u>
422 Reference Base Video Edit	Omni-Video	✓	✓	8.966	8.533	8.033	-	8.510	0.984	0.585
	InsV2V	✓	✓	5.444	5.066	5.766	-	5.425	0.978	0.608
	Ref Base Swap	✓	✓	5.033	5.966	4.966	-	5.321	0.975	0.541
	VACE	✓	✗	8.312	8.542	7.442	7.654	7.987	0.976	0.550
426 Ref Base Add	427 Ours	✓	✓	<u>9.491</u>	9.252	<u>8.375</u>	9.511	<u>9.157</u>	0.987	0.595
	Kling	✗	✓	9.714	9.571	<u>8.714</u>	<u>9.285</u>	9.321	0.992	<u>0.567</u>
	Pika	✗	✓	8.510	8.625	7.750	8.625	8.377	0.991	0.511
	VACE	✓	✗	2.665	6.540	3.052	3.636	3.973	0.987	0.561

428 4.3 COMPARSION RESULT

429 Tab. 1 and Tab. 2 respectively present the comparsion results of our method and other methods on
 430 GEdit-Bench Liu et al. (2025) and ImgEdit-Bench Ye et al. (2025a). It can be observed that our
 431 method achieves competitive performance across multiple sub-tasks, and outperforms other open-
 432 source methods in terms of the overall score on ImgEdit-Bench. Fig. 7 demonstrates that in some

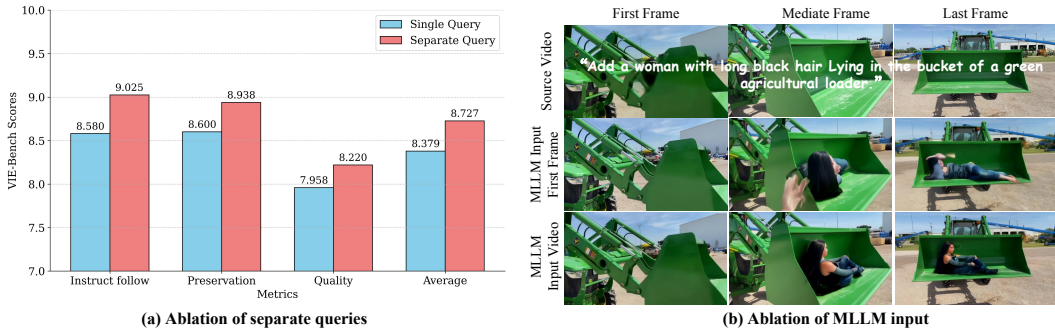


Figure 9: Ablation study of image/video independent queries (a) and MLLM inputs (b).

complex scenarios, such as removing broccoli from a cluttered pile of vegetables, methods like OmniGen Xiao et al. (2025), UniWorld Lin et al. (2025), and Step1x-Edit Liu et al. (2025) fail to recognize the target, while SeedEdit Shi et al. (2024b) and GPT-4o OpenAI produce editing results that lack consistency with the original image. Our method enables accurate removal while maintaining better consistency. Additionally, our advantages exist in cleaner background replacement and superior style consistency. We also conduct a user study in Sec. A.3 in appendix.

Table 3 shows that our method outperforms current open-source video-editing models on most metrics and remains competitive with state-of-the-art closed-source solutions. Specifically, our method attains the highest average scores on Style/Tone/Weather Change, Hybrid Edit, and Ref-Based Swap tasks among all methods, while scoring slightly below Runway Aleph on the Add, Swap/Change, and Remove tasks, and marginally below Kling on Ref-Based Add. Moreover, our method demonstrates leading advantages on several fine-grained evaluation dimensions. As shown in Fig. 8, on the fine-grained local editing task, our method achieves superior accuracy, while competing approaches either perform poorly on the handheld box replacement or fail to replace it. Our method also excels at style transfer and instruction following in hybrid edits. In reference-based editing, the backpack in our output shows higher similarity to the reference image. Additional visual comparisons are provided in Appendix Sec.A.10; we also report a user study in Appendix Sec. A.3.

4.4 ABLATION STUDY

We perform ablation studies on the design choice of unifying image and video editing: (1) whether to separate image and video queries; (2) whether the MLLM requires multi-frame video input. As shown in Fig 9 (a), the separate query setting achieves a higher score on VIE-Bench, as it better distinguishes the feature extraction for different modality information. Fig 9 (b) shows that if the MLLM only uses the first frame of the video to generate editing guidance, the editing results are prone to collapse in some complex scenarios, such as when the edited content appears in the middle of the video.

5 CONCLUSION

In this paper, we propose InstructX, a unified framework for image and video editing. Specifically, we conduct a comprehensive study on the design for the combination of MLLM and diffusion models, ultimately selecting the integration of Learnable Query, MLLM LoRA, and MLP Connector, which achieves faster convergence and superior performance. Furthermore, we explore mixed image-video training, which not only enables unified modeling for image and video editing but also expands the scope of video editing task. Additionally, we employ separate queries within the unified framework to better distinguish different modalities. We also introduce a MLLM-based video editing benchmark, *i.e.*, VIE-Bench, comprising 140 high-quality editing instances across eight categories. Extensive experiments demonstrate that our method outperforms the latest open-source image and video editing methods. Particularly, in video editing, InstructX achieves comparable performance to some closed-source editing methods while supporting a broader range of tasks.

Limitation Although InstructX demonstrates remarkable performance and appealing training efficiency, it is constrained by the pre-trained video DiT, making it difficult for high-resolution (e.g., $>1080P$) image/video editing. Although image data can excite zero-shot video editing capabilities, it is not a direct solution. However, it can serve as a temporary solution to address the current shortage of video data.

486 REFERENCES
487

488 Shuai Bai, Keqin Chen, Xuejing Liu, Jialin Wang, Wenbin Ge, Sibo Song, Kai Dang, Peng Wang,
489 Shijie Wang, Jun Tang, Humen Zhong, Yuanzhi Zhu, Mingkun Yang, Zhaohai Li, Jianqiang Wan,
490 Pengfei Wang, Wei Ding, Zheren Fu, Yiheng Xu, Jiabo Ye, Xi Zhang, Tianbao Xie, Zesen Cheng,
491 Hang Zhang, Zhibo Yang, Haiyang Xu, and Junyang Lin. Qwen2.5-vl technical report. *arXiv*
492 preprint *arXiv:2502.13923*, 2025.

493 Yuxuan Bian, Zhaoyang Zhang, Xuan Ju, Mingdeng Cao, Liangbin Xie, Ying Shan, and Qiang
494 Xu. Videopainter: Any-length video inpainting and editing with plug-and-play context control.
495 In *Proceedings of the Special Interest Group on Computer Graphics and Interactive Techniques*
496 *Conference Conference Papers*, pp. 1–12, 2025.

497 Tim Brooks, Aleksander Holynski, and Alexei A Efros. Instructpix2pix: Learning to follow image
498 editing instructions. In *Proceedings of the IEEE/CVF conference on computer vision and pattern*
499 *recognition*, pp. 18392–18402, 2023.

500 Juhai Chen, Zhiyang Xu, Xichen Pan, Yushi Hu, Can Qin, Tom Goldstein, Lifu Huang, Tianyi
501 Zhou, Saining Xie, Silvio Savarese, et al. Blip3-o: A family of fully open unified multimodal
502 models-architecture, training and dataset. *arXiv preprint arXiv:2505.09568*, 2025a.

503 Xiaokang Chen, Zhiyu Wu, Xingchao Liu, Zizheng Pan, Wen Liu, Zhenda Xie, Xingkai Yu, and
504 Chong Ruan. Janus-pro: Unified multimodal understanding and generation with data and model
505 scaling. *arXiv preprint arXiv:2501.17811*, 2025b.

506 Jiaxin Cheng, Tianjun Xiao, and Tong He. Consistent video-to-video transfer using synthetic dataset.
507 *arXiv preprint arXiv:2311.00213*, 2023.

508 Hyung Won Chung, Le Hou, Shayne Longpre, Barret Zoph, Yi Tay, William Fedus, Yunxuan Li,
509 Xuezhi Wang, Mostafa Dehghani, Siddhartha Brahma, et al. Scaling instruction-finetuned lan-
510 guage models. *Journal of Machine Learning Research*, 25(70):1–53, 2024.

511 Yuren Cong, Mengmeng Xu, Christian Simon, Shoufa Chen, Jiawei Ren, Yanping Xie, Juan-Manuel
512 Perez-Rua, Bodo Rosenhahn, Tao Xiang, and Sen He. Flatten: optical flow-guided attention for
513 consistent text-to-video editing. *arXiv preprint arXiv:2310.05922*, 2023.

514 Chaorui Deng, Deyao Zhu, Kunchang Li, Chenhui Gou, Feng Li, Zeyu Wang, Shu Zhong, Weihao
515 Yu, Xiaonan Nie, Ziang Song, et al. Emerging properties in unified multimodal pretraining. *arXiv*
516 preprint *arXiv:2505.14683*, 2025.

517 Runpei Dong, Chunrui Han, Yuang Peng, Zekun Qi, Zheng Ge, Jinrong Yang, Liang Zhao, Jianjian
518 Sun, Hongyu Zhou, Haoran Wei, Xiangwen Kong, Xiangyu Zhang, ‡Kaisheng Ma, and ¶ Li.
519 Dreamllm: Synergistic multimodal comprehension and creation.

520 Zixun Fang, Wei Zhai, Aimin Su, Hongliang Song, Kai Zhu, Mao Wang, Yu Chen, Zhiheng Liu,
521 Yang Cao, and Zheng-Jun Zha. Vivid: Video virtual try-on using diffusion models. *arXiv preprint*
522 *arXiv:2405.11794*, 2024.

523 Tsu-Jui Fu, Xin Eric Wang, Scott Grafton, Miguel Eckstein, and William Yang Wang. Sscr: Iter-
524 ative language-based image editing via self-supervised counterfactual reasoning. *arXiv preprint*
525 *arXiv:2009.09566*, 2020.

526 Tsu-Jui Fu, Wenze Hu, Xianzhi Du, William Yang Wang, Yinfei Yang, and Zhe Gan. Guid-
527 ing instruction-based image editing via multimodal large language models. *arXiv preprint*
528 *arXiv:2309.17102*, 2023.

529 Yuying Ge, Sijie Zhao, Jinguo Zhu, Yixiao Ge, Kun Yi, Lin Song, Chen Li, Xiaohan Ding, and Ying
530 Shan. Seed-x: Multimodal models with unified multi-granularity comprehension and generation.
531 *arXiv preprint arXiv:2404.14396*, 2024.

532 Ian Goodfellow, Jean Pouget-Abadie, Mehdi Mirza, Bing Xu, David Warde-Farley, Sherjil Ozair,
533 Aaron Courville, and Yoshua Bengio. Generative adversarial networks. *Communications of the*
534 *ACM*, 63(11):139–144, 2020.

540 Jonathan Ho, Ajay Jain, and Pieter Abbeel. Denoising diffusion probabilistic models. *Advances in*
 541 *neural information processing systems*, 33:6840–6851, 2020.

542

543 Edward J Hu, Yelong Shen, Phillip Wallis, Zeyuan Allen-Zhu, Yuanzhi Li, Shean Wang, Lu Wang,
 544 Weizhu Chen, et al. Lora: Low-rank adaptation of large language models. *ICLR*, 1(2):3, 2022.

545

546 Zeyinzi Jiang, Zhen Han, Chaojie Mao, Jingfeng Zhang, Yulin Pan, and Yu Liu. Vace: All-in-one
 547 video creation and editing. *arXiv preprint arXiv:2503.07598*, 2025.

548

549 Yang Jin, Kun Xu, Liwei Chen, Chao Liao, Jianchao Tan, Quzhe Huang, Bin Chen, Chenyi Lei,
 550 An Liu, Chengru Song, et al. Unified language-vision pretraining in llm with dynamic discrete
 551 visual tokenization. *arXiv preprint arXiv:2309.04669*, 2023.

552

553 Keling. Image to video elements feature. <https://app.klingai.com/cn/multimodal-to-video/add-object/new>, 2025.

554

555 Max Ku, Cong Wei, Weiming Ren, Harry Yang, and Wenhui Chen. Anyv2v: A tuning-free frame-
 556 work for any video-to-video editing tasks. *arXiv preprint arXiv:2403.14468*, 2024.

557

558 Maksim Kuprashevich, Grigorii Alekseenko, Irina Tolstykh, Georgii Fedorov, Bulat Suleimanov,
 559 Vladimir Dokholyan, and Aleksandr Gordeev. NoHumansRequired: Autonomous High-Quality
 560 Image Editing Triplet Mining. *arXiv preprint arXiv:2507.14119*, 2025. URL <https://arxiv.org/abs/2507.14119>.

561

562 Black Forest Labs, Stephen Batifol, Andreas Blattmann, Frederic Boesel, Saksham Consul, Cyril
 563 Diagne, Tim Dockhorn, Jack English, Zion English, Patrick Esser, et al. Flux. 1 kontext:
 564 Flow matching for in-context image generation and editing in latent space. *arXiv preprint
 565 arXiv:2506.15742*, 2025.

566

567 Doyup Lee, Chiheon Kim, Saehoon Kim, Minsu Cho, and Wook-Shin Han. Autoregressive image
 568 generation using residual quantization. In *Proceedings of the IEEE/CVF conference on computer
 569 vision and pattern recognition*, pp. 11523–11532, 2022.

570

571 Bowen Li, Xiaojuan Qi, Thomas Lukasiewicz, and Philip HS Torr. Manigan: Text-guided image
 572 manipulation. In *Proceedings of the IEEE/CVF conference on computer vision and pattern recog-
 573 nition*, pp. 7880–7889, 2020.

574

575 Junnan Li, Dongxu Li, Silvio Savarese, and Steven Hoi. Blip-2: Bootstrapping language-image
 576 pre-training with frozen image encoders and large language models. In *International conference
 577 on machine learning*, pp. 19730–19742. PMLR, 2023.

578

579 Xiaowen Li, Haolan Xue, Peiran Ren, and Liefeng Bo. Diffueraser: A diffusion model for video
 580 inpainting, 2025. URL <https://arxiv.org/abs/2501.10018>.

581

582 Sen Liang, Zhenqiao Yu, Zhengguang Zhou, Teng Hu, Hongmei Wang, Yi Chen, Qin Lin, Yuan
 583 Zhou, Xin Li, Qinglin Lu, et al. Omniv2v: Versatile video generation and editing via dynamic
 584 content manipulation. *arXiv preprint arXiv:2506.01801*, 2025.

585

586 Bin Lin, Zongjian Li, Xinhua Cheng, Yuwei Niu, Yang Ye, Xianyi He, Shanghai Yuan, Wangbo Yu,
 587 Shaodong Wang, Yunyang Ge, et al. Uniworld: High-resolution semantic encoders for unified
 588 visual understanding and generation. *arXiv preprint arXiv:2506.03147*, 2025.

589

590 Yaron Lipman, Ricky TQ Chen, Heli Ben-Hamu, Maximilian Nickel, and Matt Le. Flow matching
 591 for generative modeling. *arXiv preprint arXiv:2210.02747*, 2022.

592

593 Shilong Liu, Zhaoyang Zeng, Tianhe Ren, Feng Li, Hao Zhang, Jie Yang, Chunyuan Li, Jianwei
 594 Yang, Hang Su, Jun Zhu, et al. Grounding dino: Marrying dino with grounded pre-training for
 595 open-set object detection. *arXiv preprint arXiv:2303.05499*, 2023.

596

597 Shiyu Liu, Yucheng Han, Peng Xing, Fukun Yin, Rui Wang, Wei Cheng, Jiaqi Liao, Yingming
 598 Wang, Honghao Fu, Chunrui Han, et al. Step1x-edit: A practical framework for general image
 599 editing. *arXiv preprint arXiv:2504.17761*, 2025.

594 Jiasen Lu, Christopher Clark, Sangho Lee, Zichen Zhang, Savya Khosla, Ryan Marten, Derek
 595 Hoiem, and Aniruddha Kembhavi. Unified-io 2: Scaling autoregressive multimodal models with
 596 vision, language, audio, and action. Dec 2023.

597

598 Jian Ma, Xujie Zhu, Zihao Pan, Qirong Peng, Xu Guo, Chen Chen, and Haonan Lu. X2edit: Revis-
 599 iting arbitrary-instruction image editing through self-constructed data and task-aware representa-
 600 tion learning, 2025a. URL <https://arxiv.org/abs/2508.07607>.

601 Yiyang Ma, Xingchao Liu, Xiaokang Chen, Wen Liu, Chengyue Wu, Zhiyu Wu, Zizheng Pan,
 602 Zhenda Xie, Haowei Zhang, Xingkai Yu, et al. Janusflow: Harmonizing autoregression and rec-
 603 tified flow for unified multimodal understanding and generation. In *Proceedings of the Computer
 604 Vision and Pattern Recognition Conference*, pp. 7739–7751, 2025b.

605

606 Chong Mou, Mingdeng Cao, Xintao Wang, Zhaoyang Zhang, Ying Shan, and Jian Zhang. Revideo:
 607 Remake a video with motion and content control. *Advances in Neural Information Processing
 608 Systems*, 37:18481–18505, 2024.

609 Seonghyeon Nam, Yunji Kim, and Seon Joo Kim. Text-adaptive generative adversarial networks:
 610 manipulating images with natural language. *Advances in neural information processing systems*,
 611 31, 2018.

612 OpenAI. Introducing gpt-4o: Image generation. URL <https://openai.com/index/introducing-4o-image-generation/>.

613

614 Wenqi Ouyang, Yi Dong, Lei Yang, Jianlou Si, and Xingang Pan. I2vedit: First-frame-guided video
 615 editing via image-to-video diffusion models. In *SIGGRAPH Asia 2024 Conference Papers*, pp.
 616 1–11, 2024.

617

618 Xichen Pan, Satya Narayan Shukla, Aashu Singh, Zhuokai Zhao, Shlok Kumar Mishra, Jialiang
 619 Wang, Zhiyang Xu, Juhai Chen, Kunpeng Li, Felix Juefei-Xu, et al. Transfer between modalities
 620 with metaqueries. *arXiv preprint arXiv:2504.06256*, 2025.

621

622 Pika. Pikaadd. <https://pika.art/pikadditions>, 2025.

623

624 Jordi Pont-Tuset, Federico Perazzi, Sergi Caelles, Pablo Arbeláez, Alex Sorkine-Hornung, and
 625 Luc Van Gool. The 2017 davis challenge on video object segmentation. *arXiv preprint
 626 arXiv:1704.00675*, 2017.

627

628 Chenyang Qi, Xiaodong Cun, Yong Zhang, Chenyang Lei, Xintao Wang, Ying Shan, and Qifeng
 629 Chen. Fatezero: Fusing attentions for zero-shot text-based video editing. In *Proceedings of the
 630 IEEE/CVF International Conference on Computer Vision*, pp. 15932–15942, 2023.

631

632 Liao Qu, Huichao Zhang, Yiheng Liu, Xu Wang, Yi Jiang, Yiming Gao, Hu Ye, Daniel K Du, Ze-
 633 huan Yuan, and Xinglong Wu. Tokenflow: Unified image tokenizer for multimodal understanding
 634 and generation. In *Proceedings of the Computer Vision and Pattern Recognition Conference*, pp.
 2545–2555, 2025.

635

636 Nikhila Ravi, Valentin Gabeur, Yuan-Ting Hu, Ronghang Hu, Chaitanya Ryali, Tengyu Ma, Haitham
 637 Khedr, Roman Rädle, Chloe Rolland, Laura Gustafson, Eric Mintun, Junting Pan, Kalyan Va-
 638 sudev Alwala, Nicolas Carion, Chao-Yuan Wu, Ross Girshick, Piotr Dollár, and Christoph Fe-
 639 ichtenhofer. Sam 2: Segment anything in images and videos. *arXiv preprint arXiv:2408.00714*,
 2024. URL <https://arxiv.org/abs/2408.00714>.

640

641 Nataniel Ruiz, Yuanzhen Li, Varun Jampani, Yael Pritch, Michael Rubinstein, and Kfir Aberman.
 642 Dreambooth: Fine tuning text-to-image diffusion models for subject-driven generation. In *Pro-
 643 ceedings of the IEEE/CVF Conference on Computer Vision and Pattern Recognition*, 2023.

644

645 Runway. Creating anything. <https://runwayml.com/>, 2025.

646

647 Weijia Shi, Xiaochuang Han, Chunting Zhou, Weixin Liang, Xi Victoria Lin, Luke Zettlemoyer,
 648 and Lili Yu. Lmfusion: Adapting pretrained language models for multimodal generation. *arXiv
 649 preprint arXiv:2412.15188*, 2024a.

648 Yichun Shi, Peng Wang, and Weilin Huang. Seededit: Align image re-generation to image editing.
 649 *arXiv preprint arXiv:2411.06686*, 2024b.
 650

651 Quan Sun, Qiying Yu, Yufeng Cui, Fan Zhang, Xiaosong Zhang, Yueze Wang, Hongcheng Gao,
 652 Jingjing Liu, Tiejun Huang, and Xinlong Wang. Emu: Generative pretraining in multimodality.
 653 *arXiv preprint arXiv:2307.05222*, 2023.

654 Quan Sun, Yufeng Cui, Xiaosong Zhang, Fan Zhang, Qiying Yu, Yueze Wang, Yongming Rao,
 655 Jingjing Liu, Tiejun Huang, and Xinlong Wang. Generative multimodal models are in-context
 656 learners. In *Proceedings of the IEEE/CVF Conference on Computer Vision and Pattern Recog-
 657 nition*, pp. 14398–14409, 2024.

658 Zhiyu Tan, Hao Yang, Luozheng Qin, Jia Gong, Mengping Yang, and Hao Li. Omni-video: Democ-
 659 ratizing unified video understanding and generation. *arXiv preprint arXiv:2507.06119*, 2025.
 660

661 Chameleon Team. Chameleon: Mixed-modal early-fusion foundation models, 2024. *URL
 662 https://arxiv.org/abs/2405.09818*, 9(8), 2024.

663 Shengbang Tong, David Fan, Jiachen Zhu, Yunyang Xiong, Xinlei Chen, Koustuv Sinha, Michael
 664 Rabbat, Yann LeCun, Saining Xie, and Zhuang Liu. Metamorph: Multimodal understanding and
 665 generation via instruction tuning. *arXiv preprint arXiv:2412.14164*, 2024.

666 Yuanpeng Tu, Hao Luo, Xi Chen, Sihui Ji, Xiang Bai, and Hengshuang Zhao. Videoanydoor: High-
 667 fidelity video object insertion with precise motion control. In *Proceedings of the Special Interest
 668 Group on Computer Graphics and Interactive Techniques Conference Papers*, pp.
 669 1–11, 2025.

670 Team Wan, Ang Wang, Baole Ai, Bin Wen, Chaojie Mao, Chen-Wei Xie, Di Chen, Feiwu Yu,
 671 Haiming Zhao, Jianxiao Yang, Jianyuan Zeng, Jiayu Wang, Jingfeng Zhang, Jingren Zhou, Jinkai
 672 Wang, Jixuan Chen, Kai Zhu, Kang Zhao, Keyu Yan, Lianghua Huang, Mengyang Feng, Ningyi
 673 Zhang, Pandeng Li, Pingyu Wu, Ruihang Chu, Ruili Feng, Shiwei Zhang, Siyang Sun, Tao Fang,
 674 Tianxing Wang, Tianyi Gui, Tingyu Weng, Tong Shen, Wei Lin, Wei Wang, Wei Wang, Wenmeng
 675 Zhou, Wente Wang, Wenting Shen, Wenyuan Yu, Xianzhong Shi, Xiaoming Huang, Xin Xu, Yan
 676 Kou, Yangyu Lv, Yifei Li, Yijing Liu, Yiming Wang, Yingya Zhang, Yitong Huang, Yong Li, You
 677 Wu, Yu Liu, Yulin Pan, Yun Zheng, Yuntao Hong, Yupeng Shi, Yutong Feng, Zeyinzi Jiang, Zhen
 678 Han, Zhi-Fan Wu, and Ziyu Liu. Wan: Open and advanced large-scale video generative models.
 679 *arXiv preprint arXiv:2503.20314*, 2025.

680 Bryan Wang, Yuliang Li, Zhaoyang Lv, Haijun Xia, Yan Xu, and Raj Sodhi. Lave: Llm-powered
 681 agent assistance and language augmentation for video editing. In *Proceedings of the 29th Inter-
 682 national Conference on Intelligent User Interfaces*, pp. 699–714, 2024a.

683 Qiuhe Wang, Yukai Shi, Jiarong Ou, Rui Chen, Ke Lin, Jiahao Wang, Boyuan Jiang, Haotian
 684 Yang, Mingwu Zheng, Xin Tao, et al. Koala-36m: A large-scale video dataset improving consis-
 685 tency between fine-grained conditions and video content. In *Proceedings of the Computer Vision
 686 and Pattern Recognition Conference*, pp. 8428–8437, 2025a.

687 Yuhan Wang, Siwei Yang, Bingchen Zhao, Letian Zhang, Qing Liu, Yuyin Zhou, and Cihang
 688 Xie. Gpt-image-edit-1.5 m: A million-scale, gpt-generated image dataset. *arXiv preprint
 689 arXiv:2507.21033*, 2025b.

690 Zhenzhi Wang, Yixuan Li, Yanhong Zeng, Youqing Fang, Yuwei Guo, Wenran Liu, Jing Tan, Kai
 691 Chen, Tianfan Xue, Bo Dai, and Dahu Lin. Humanvid: Demystifying training data for camera-
 692 controllable human image animation. In *NeurIPS*, 2024b.

693 Chenyuan Wu, Pengfei Zheng, Ruiran Yan, Shitao Xiao, Xin Luo, Yueze Wang, Wanli Li, Xiyan
 694 Jiang, Yixin Liu, Junjie Zhou, et al. Omnigen2: Exploration to advanced multimodal generation.
 695 *arXiv preprint arXiv:2506.18871*, 2025.

696 Jay Zhangjie Wu, Yixiao Ge, Xintao Wang, Stan Weixian Lei, Yuchao Gu, Yufei Shi, Wynne Hsu,
 697 Ying Shan, Xiaohu Qie, and Mike Zheng Shou. Tune-a-video: One-shot tuning of image diffusion
 698 models for text-to-video generation. In *Proceedings of the IEEE/CVF International Conference
 699 on Computer Vision*, pp. 7623–7633, 2023.

702 Shitao Xiao, Yueze Wang, Junjie Zhou, Huaying Yuan, Xingrun Xing, Ruiran Yan, Chaofan Li,
 703 Shuting Wang, Tiejun Huang, and Zheng Liu. Omnigen: Unified image generation. In *Proceed-
 704 ings of the Computer Vision and Pattern Recognition Conference*, pp. 13294–13304, 2025.

705 Jinpeng Xie, Weijia Mao, Zechen Bai, David Junhao Zhang, Weihao Wang, Kevin Qinghong Lin,
 706 Yuchao Gu, Zhijie Chen, Zhenheng Yang, and Mike Zheng Shou. Show-o: One single transformer
 707 to unify multimodal understanding and generation. *arXiv preprint arXiv:2408.12528*, 2024.

708 Zhendong Yang, Ailing Zeng, Chun Yuan, and Yu Li. Effective whole-body pose estimation with
 709 two-stages distillation. In *Proceedings of the IEEE/CVF International Conference on Computer
 710 Vision*, pp. 4210–4220, 2023.

711 Yang Ye, Xianyi He, Zongjian Li, Bin Lin, Shenghai Yuan, Zhiyuan Yan, Bohan Hou, and Li Yuan.
 712 Imgedit: A unified image editing dataset and benchmark. *arXiv preprint arXiv:2505.20275*,
 713 2025a.

714 Zixuan Ye, Xuanhua He, Quande Liu, Qiulin Wang, Xintao Wang, Pengfei Wan, Di Zhang, Kun
 715 Gai, Qifeng Chen, and Wenhan Luo. Unic: Unified in-context video editing. *arXiv preprint
 716 arXiv:2506.04216*, 2025b.

717 Jiahui Yu, Xin Li, Jing Yu Koh, Han Zhang, Ruoming Pang, James Qin, Alexander Ku, Yuanzhong
 718 Xu, Jason Baldridge, and Yonghui Wu. Vector-quantized image modeling with improved vqgan.
 719 *arXiv preprint arXiv:2110.04627*, 2021.

720 Shoubin Yu, Difan Liu, Ziqiao Ma, Yicong Hong, Yang Zhou, Hao Tan, Joyce Chai, and Mohit
 721 Bansal. Veggie: Instructional editing and reasoning of video concepts with grounded generation.
 722 *arXiv preprint arXiv:2503.14350*, 2025.

723 Ziyun Zeng, Junhao Zhang, Wei Li, and Mike Zheng Shou. Draw-in-mind: Learning precise image
 724 editing via chain-of-thought imagination. *arXiv preprint arXiv:2509.01986*, 2025.

725 Fan Zhang, Shulin Tian, Ziqi Huang, Yu Qiao, and Ziwei Liu. Evaluation agent: Efficient and
 726 promptable evaluation framework for visual generative models. *arXiv preprint arXiv:2412.09645*,
 727 2024a.

728 Shu Zhang, Xinyi Yang, Yihao Feng, Can Qin, Chia-Chih Chen, Ning Yu, Zeyuan Chen, Huan
 729 Wang, Silvio Savarese, Stefano Ermon, et al. Hive: Harnessing human feedback for instructional
 730 visual editing. In *Proceedings of the IEEE/CVF Conference on Computer Vision and Pattern
 731 Recognition*, pp. 9026–9036, 2024b.

732 Chunting Zhou, Lili Yu, Arun Babu, Kushal Tirumala, Michihiro Yasunaga, Leonid Shamis, Jacob
 733 Kahn, Xuezhe Ma, Luke Zettlemoyer, and Omer Levy. Transfusion: Predict the next token and
 734 diffuse images with one multi-modal model. *arXiv preprint arXiv:2408.11039*, 2024.

735 Shaobin Zhuang, Zhipeng Huang, Binxin Yang, Ying Zhang, Fangyikang Wang, Canmiao Fu,
 736 Chong Sun, Zheng-Jun Zha, Chen Li, and Yali Wang. Get in video: Add anything you want
 737 to the video. *arXiv preprint arXiv:2503.06268*, 2025.

738 Bojia Zi, Weixuan Peng, Xianbiao Qi, Jianan Wang, Shihao Zhao, Rong Xiao, and Kam-Fai
 739 Wong. Minimax-remover: Taming bad noise helps video object removal. *arXiv preprint
 740 arXiv:2505.24873*, 2025a.

741 Bojia Zi, Penghui Ruan, Marco Chen, Xianbiao Qi, Shaozhe Hao, Shihao Zhao, Youze Huang, Bin
 742 Liang, Rong Xiao, and Kam-Fai Wong. Se\`norita-2m: A high-quality instruction-based dataset
 743 for general video editing by video specialists. *arXiv preprint arXiv:2502.06734*, 2025b.

744 Bojia Zi, Shihao Zhao, Xianbiao Qi, Jianan Wang, Yukai Shi, Qianyu Chen, Bin Liang, Rong Xiao,
 745 Kam-Fai Wong, and Lei Zhang. Cococo: Improving text-guided video inpainting for better con-
 746 sistency, controllability and compatibility. In *Proceedings of the AAAI Conference on Artificial
 747 Intelligence*, volume 39, pp. 11067–11076, 2025c.

748 Tongchun Zuo, Zaiyu Huang, Shuliang Ning, Ente Lin, Chao Liang, Zerong Zheng, Jianwen Jiang,
 749 Yuan Zhang, Mingyuan Gao, and Xin Dong. Dreamvvt: Mastering realistic video virtual try-on
 750 in the wild via a stage-wise diffusion transformer framework. *arXiv preprint arXiv:2508.02807*,
 751 2025.

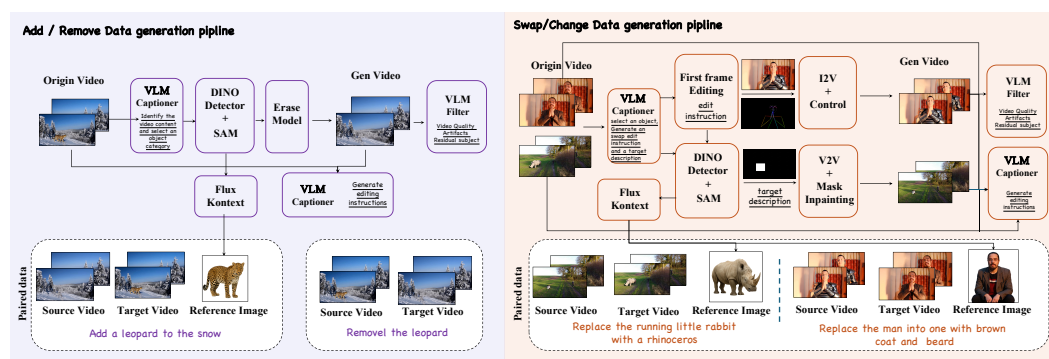
752

756 **A APPENDIX**
757758 **A.1 VIE-BENCHMARK DETAILS**

759 As discussed in Sec. 4.2, given the scarcity of public video editing benchmarks, we build a high-
760 quality, instruction-based video editing benchmark. Specifically, The source videos come from pub-
761 lic datasets (*e.g.*, DAVIS Pont-Tuset et al. (2017), HumanVid Wang et al. (2024b)) and the web. All
762 videos are 720P and 3–10 seconds long, covering indoor, outdoor, dynamic, animated, and portrait
763 scenes. For each video, we used GPT-4o to generate 5 editing instructions, followed by careful
764 manual curation to ensure that the instructions align with the original video content while retaining
765 a degree of creativity. For reference-based editing tasks, the reference images are derived from the
766 DreamBooth Ruiz et al. (2023) dataset. In total, our benchmark comprises eight fine-grained video-
767 editing tasks with 140 editing examples. As shown in Tab. 4. The benchmark encompasses local
768 video editing tasks—add, object swap, color change, and remove; global editing tasks—style change
769 and tone/weather change; and reference base tasks—including reference base add and reference base
770 swap.

771 **A.2 VIDEO SYNTHESIS PAIRED DATA PIPELINE**

772 To construct high-quality paired training data for video editing, we develop a synthetic video-editing
773 data pipeline covering the editing tasks: add, reference-based add, remove, swap, and reference-
774 based swap. Source videos are drawn from Wang et al. (2025a). We use PySceneDetect to partition
775 videos into single-scene clips, which serve as the original video. The data synthesis pipeline is
776 shown in Fig. 10.

790 Figure 10: Pipeline for synthesizing paired video data.
791793 Table 4: Editing Tasks in VIE-Bench.
794

795 Edit Task	796 Sub Edit Task	797 Number
Total		140
800 Local Edit	Object Swap	25
	Color Change	10
	Add	30
	Remove	30
805 Global Edit	Style Change	10
	Tone / Weather Change	5
Hybrid Edit		10
810 Reference Base Edit	Reference Base Swap	10
	Reference Base Add	10

808 For the add and remove data. We first employ GPT-4o to analyze the video and identify a target
809 subject category. Leveraging Grounding DINO Liu et al. (2023) and SAM Ravi et al. (2024), we

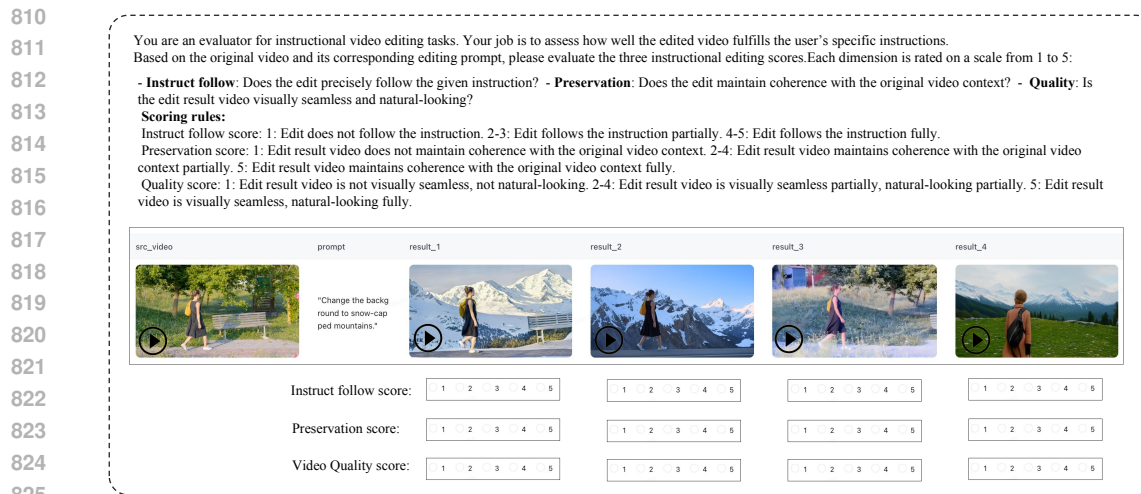


Figure 11: User study example.

segment the corresponding masks and then apply video erasure techniques Zi et al. (2025a) to remove the target subjects, with a MLLM-based filtering mechanism that avoids visual artifacts of inpainting. The original and erased videos are subsequently provided to GPT-4o. By swapping the roles of the original and generated videos, GPT-4o is prompted to produce “remove” and “add” editing instructions. We use Flux-Kontext Labs et al. (2025) to generate cross-pair reference images of the edit object, to form quadruples—source video, target video, reference image, and instruction prompt. Finally, the training set comprised 65K removal paired samples and 73K add paired samples.

For the swap and change data, we first apply an optical-flow-based analysis to partition videos into static-background and dynamic-background categories. Paired editing data are synthesized via two routes. First, we use GPT-4o to select a target subject category and to generate both the editing instruction and the target prompt. For human-centric, static-background videos, Flux-Kontext produces the edited first-frame image. Pose sequences of the characters are extracted with DW-pose Yang et al. (2023), after which a pose-driven image-to-video expert model generates a driven video used as the source video. The original video is treated as the target video, and these are provided to GPT-4o to obtain editing instructions. Additionally, we segment the target object in the first frame and use Flux-Kontext to generate cross-pair reference images of the edited target object, yielding paired training data composed of the source video, target video, reference image, and instruction prompt. For dynamic-background editing, a specially trained, mask-based video inpainting expert model is employed during video generation to construct editing triplets, ensuring consistency under substantial background changes and motion. We ultimately used 98K paired swap/change samples as training data.

A.3 USER STUDY

We invited 30 professional image and video creators to serve as our user evaluation experts. For the image-editing tasks, we randomly selected 30 image-editing sample pairs from GEdit-Bench and 30 from ImgEdit-Bench, for a total of 60 pairs. For the video-editing tasks, we randomly selected 60 non-reference video-editing samples from VIE-bench. Our user study example is shown in Fig.11. Users rated 8 image-editing methods and 4 instruct-based video-editing methods on three dimensions, including ‘Instruct follow’, ‘Preservation’ and ‘Quality’. All scores range from 1 to 5, and we averaged the ratings to obtain the final scores. The user study was carried out under blinded to reduce bias and promote fairness. Figs.12 and 13 indicate that our method outperforms current open source image and video editing methods in the user study and is competitive with the state-of-the-art closed source solution.

A.4 MORE ABLATION STUDIES

The impact of image data. In Fig. 6 of the main paper, we demonstrate that the model can perform untrained video editing tasks under mixed image-video training. To further verify that this

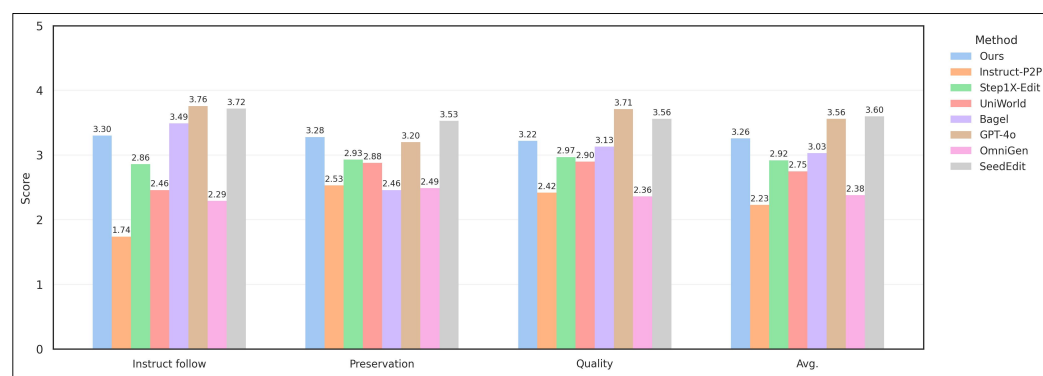


Figure 12: User study result of image edit.

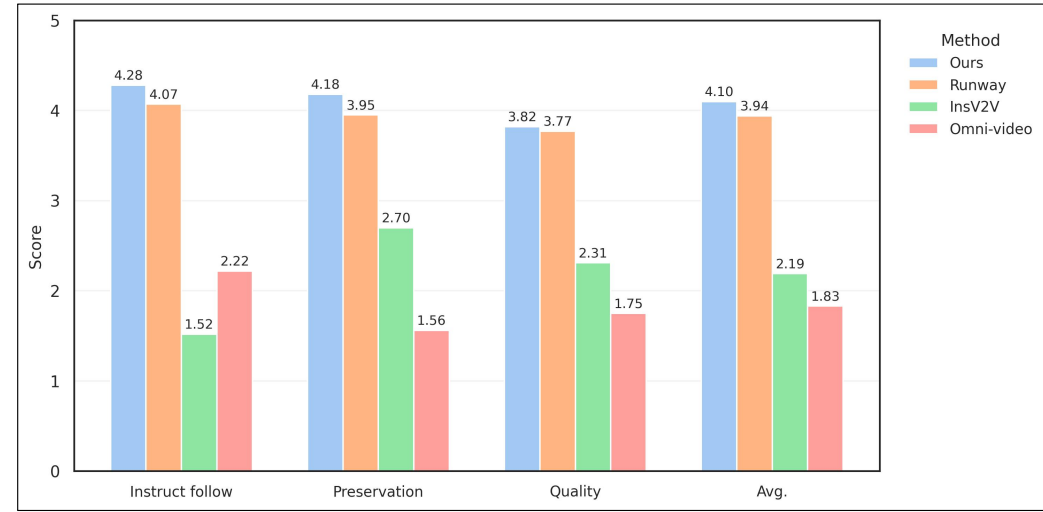


Figure 13: User study result of video edit.

improvement comes from the image data, Fig. 14 compares the editing results from training with both image and video data against those from training with video data alone. Note that the video data does not include training data for segmentation and style transfer. It can be seen that training without mixed image data fails to enable zero-shot video editing tasks. Furthermore, in Tab. 5, we present the impact of the image-video training mixture ratio on model performance, which shows insensitivity to the mixing ratio.

The impact of video data. The results in Fig. 15 demonstrate that using only image data disrupts the temporal consistency of video generation outcomes, leading to undesired flickering and artifacts. Moreover, the video editing performance obtained using only image training data are also unsatisfactory.

The number of video queries. In the main paper, Fig. 9(a) verifies the performance gain achieved by utilizing modality-independent queries. In this part, we further study the impact of the number of queries on performance. Specifically, we double the number of video queries. Tab. 6 indicates that an excessive number of queries does not yield a significant performance improvement, primarily because the VLM mainly provides high-level semantic information.

A.5 LONG VIDEO EDITING PIPELINE

Our InstructX can also perform long video editing by modifying the inference pipeline. Specifically, we process long videos using a sliding window approach, where consecutive windows overlap at the tail frame of the previous window and the head frame of the next window. During editing, the editing result of the tail frame of the preceding window replaces the head frame of the subsequent

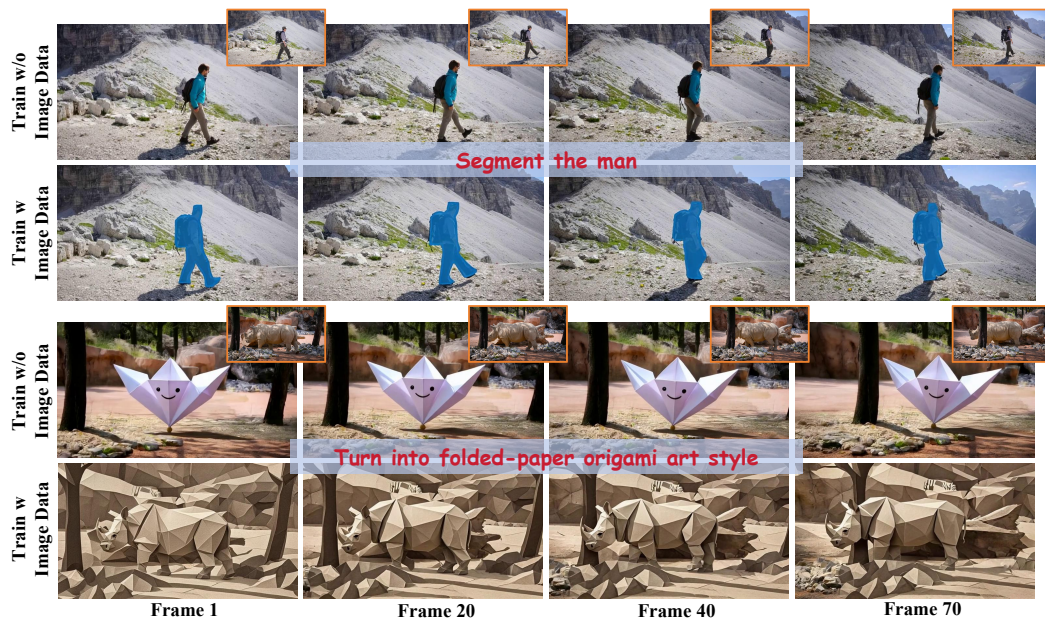


Figure 14: Comparison of zero-shot video editing capabilities with and without image training data. The first row demonstrates video segmentation, while the second row showcases video stylization.

Table 5: The impact of different image-video training mixture ratios on video editing performance.

image:video	5,000 iter			10,000 iter		
	Instruct follow	Preservation	Quality	Instruct follow	Preservation	Quality
2:3 (paper setting)	8.40	8.73	7.77	8.26	8.73	7.59
1:4	8.36	8.74	7.67	7.91	8.54	7.38
4:1	8.41	8.79	7.74	8.69	8.92	7.87

window to maintain consistency between windows. During testing, we use a 5-second window. Fig. 16 demonstrates the editing results for a 30-second, 30 FPS video. It can be observed that the transitions between windows are smooth. Therefore, our method can be extended to long video editing.

A.6 HIGH-RESOLUTION VIDEO EDITING

Although we use 480P resolution data during training, we found that the model also has generalization capability for higher resolutions. Fig. 17 demonstrates the promising editing results at 1080P resolution.

A.7 MORE DETAILS OF MODEL SIZE

In Tab. 7, we present the model size of representative image editing and video editing methods. It can be seen that the number of model parameters in our method is comparable to that of main-

Table 6: Ablation study of the number of video queries.

	5,000 iter			10,000 iter		
	Instruct follow	Preservation	Quality	Instruct follow	Preservation	Quality
512 video query	8.61	8.82	7.94	8.55	8.81	7.90
1024 video query	8.85	8.98	8.10	8.70	8.91	8.02



Replace the blackswan with a white cat

Figure 15: Video editing performance of InstructX trained solely on image editing data.



Figure 16: The performance of InstructX in long video (30s) editing using a sliding window approach.

stream approaches. The comparison in this paper demonstrate that our performance surpasses these methods.

Table 7: Model size of different methods

Method	Model Size
OmniGen	3.8B
Step1X-Edit	12.5B
UniWorld	12B
Bagel	14.6B
Omni-Video	11B
VACE	14B
ours	14B (DiT) + 0.6B (MLLM LoRA)

A.8 FURTHER DISCUSSION ON THE GAINS OF MLLM

In Fig. 18, we visualize the understanding ability gains of MLLM in visual editing. It can be observed that using only the diffusion model fails to comprehend some complex and tiny details, such as the books on the corner shelf and the plants in the corner. MLLM, however, can understand these elements quite well. In Fig. 19, we quantify the performance of using only diffusion for instruction-based editing versus MLLM+Diffusion across various tasks on ImgEdit-Bench Ye et al. (2025a). A noticeable gap can also be observed.

A.9 MLLM-BASED JUDGE

We employ GPT-4o as MLLM-based judge. Figs.20 and 21 present the MLLM scoring prompts used in our paper for the video-editing and reference-based video-editing tasks respectively.

A.10 MORE EXAMPLES

We show additional visual results in Figs. 22 - 27 .



Figure 17: The editing performance of InstructX on 1080P videos.

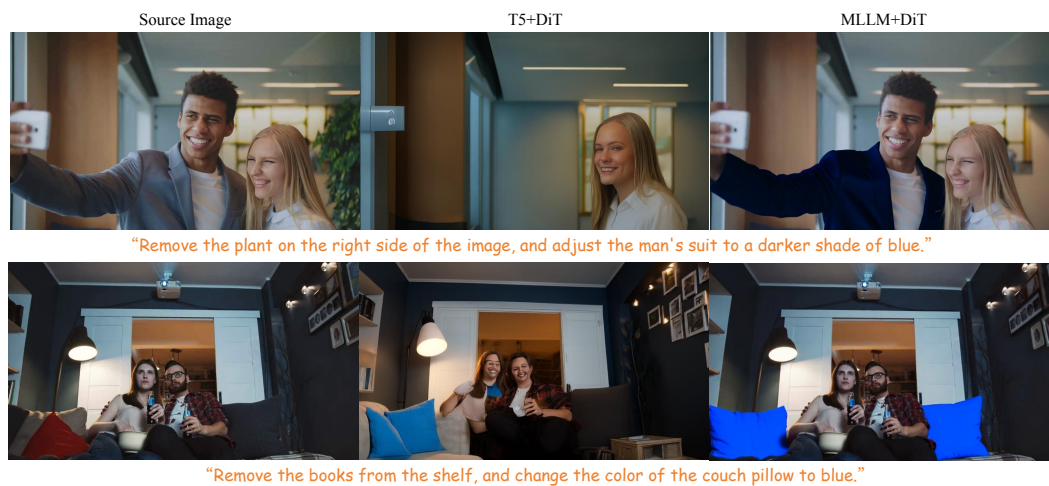


Figure 18: Comparison of understanding abilities between MLLM+Diffusion and Diffusion-only setting in instructional editing tasks.

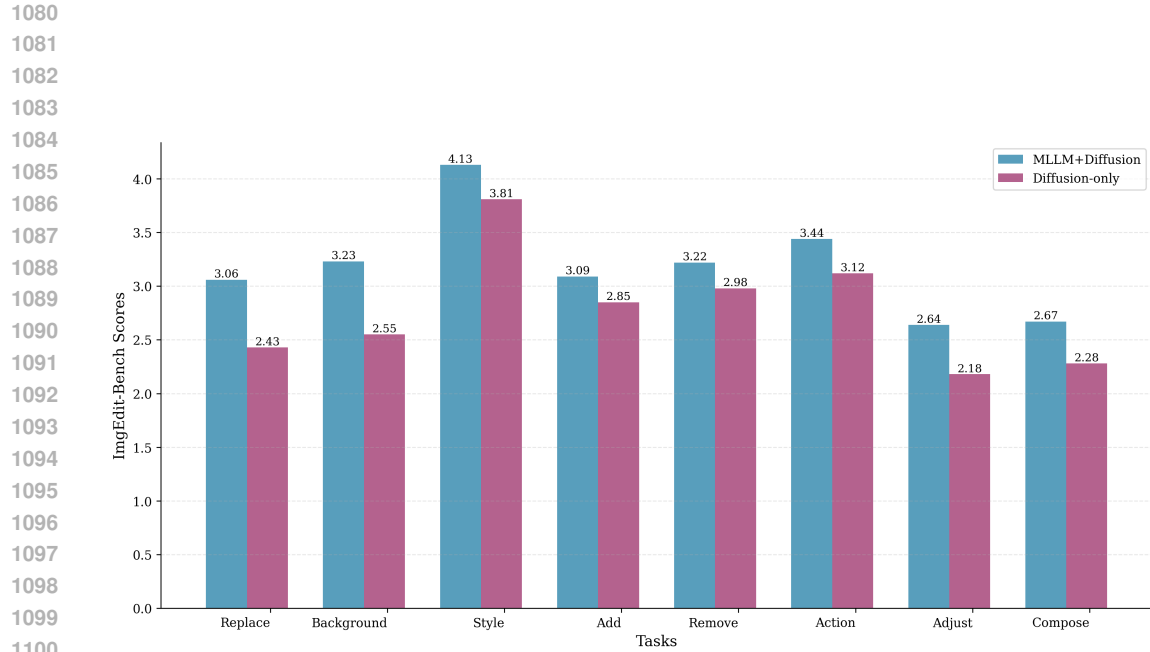


Figure 19: Comparison of understanding abilities between MLLM+Diffusion and Diffusion-only setting in instructional editing tasks.

```

1112
1113     """
1114     # **Role**
1115     You are an evaluator for instructional video editing tasks. Your job is to assess how well the edited video fulfills the user's specific instructions.
1116     # **Input**
1117     1. The user's instruction
1118     2. The original video (first video)
1119     3. The edited video (second video)
1120
1121     # **Task**
1122     Please evaluate the instruct editing score:
1123     - Instruct follow: Does the edit precisely follow the given instruction? - Quality: Is the edit result video visually seamless and natural-looking? - Preservation: Does the
1124     edit maintain coherence with the original video context?
1125     Scoring rules:
1126     Instruct follow score: 1-3: Edit does not follow the instruction. 4-6: Edit follows the instruction partially. 7-10: Edit follows the instruction fully.
1127     Quality score: 1-3: Edit result video is not visually seamless, not natural-looking and not aesthetics. 4-6: Edit result video is visually seamless partially, natural-looking
1128     partially, and aesthetics partially. 7-10: Edit result video is visually seamless fully, natural-looking fully, and aesthetics fully.
1129     Preservation score: 1-3: Edit result video does not maintain coherence with the original video context. 4-6: Edit result video maintains coherence with the original video
1130     context partially. 7-10: Edit result video maintains coherence with the original video context fully.
1131     Using the following Output format:
1132
1133     # **Output**
1134     Structure the output in JSON format with:
1135     - instruction: Repeat the user's instruction.
1136     - instruct follow score (1-10): Your score number
1137     - quality score (1-10): Your score number
1138     - preservation score (1-10): Your score number
1139     - reason: The reasons for the score you gave
1140     """

```

Figure 20: MLLM score system prompt for video edit.

```

1134
1135
1136
1137
1138
1139
1140
1141
1142
1143
1144
1145
1146
1147
1148
1149
1150
1151
1152
1153
1154
1155
1156
1157
1158
1159
1160
1161
1162
1163
1164
1165
1166
1167
1168
1169
1170
1171
1172
1173
1174
1175
1176
1177
1178
1179
1180
1181
1182
1183
1184
1185
1186
1187

```

**Role**
You are an evaluator for instructional video editing tasks. Your job is to assess how well the edited video fulfills the user's specific instructions.

**Input**
1. The user's instruction
2. The reference image.
2. The original video (first video)
3. The edited video (second video)

**Task**
Please evaluate the reference base instruct editing score: - **Instruct follow**: Does the edit precisely follow the given instruction? - **Quality**: Is the edit result video visually seamless and natural-looking? - **Preservation**: Does the edit maintain coherence with the original video context? - **Similarity**: The similarity between the editing object in edited video(replace or add) and the reference image?
Scoring rules:
Instruct follow score: 1-3: Edit does not follow the instruction. 4-6: Edit follows the instruction partially. 7-10: Edit follows the instruction fully.
Quality score: 1-3: Edit result video is not visually seamless, not natural-looking and not aesthetics. 4-6: Edit result video is visually seamless partially, natural-looking partially, and aesthetics partially. 7-10: Edit result video is visually seamless fully, natural-looking fully, and aesthetics fully.
Preservation score: 1-3: Edit result video does not maintain coherence with the original video context. 4-6: Edit result video maintains coherence with the original video context partially. 7-10: Edit result video maintains coherence with the original video context fully.
Similarity score: 1-3: In the edited video (replaced or added), the similarity between the edited object and the reference image is low. 4-6: the similarity is medium . 7-10: the similarity is high.
Using the following Output format:

**Output**
Structure the output in JSON format with:
- instruction: Repeat the user's instruction.
- instruct follow score (1-10): Your score number
- quality score (1-10): Your score number
- preservation score (1-10): Your score number
- similarity score (1-10): Your score number
- reason: The reasons for the score you gave

Figure 21: MLLM score system prompt for reference base video edit.

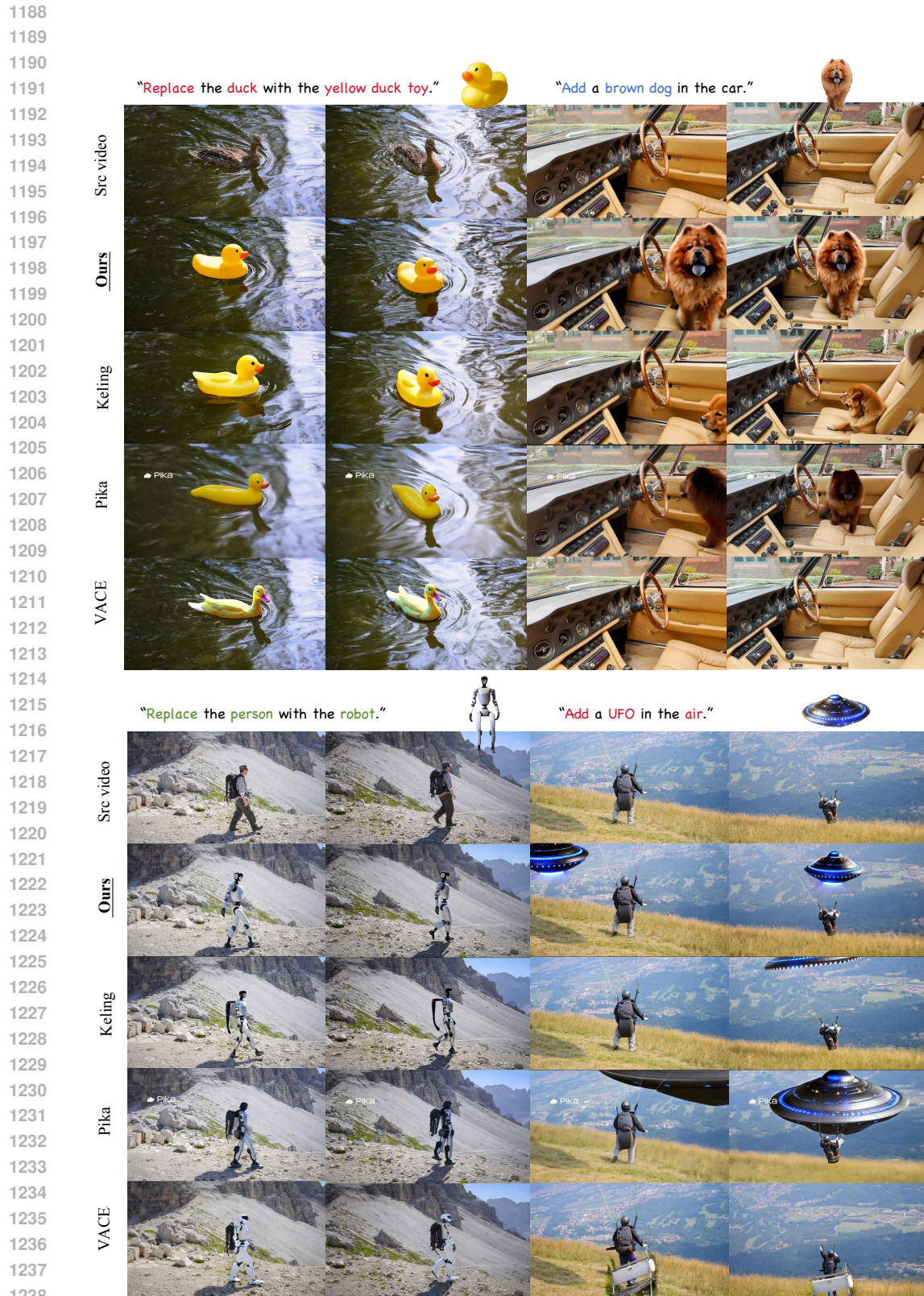


Figure 22: Visual comparsion on VIE-Bench.

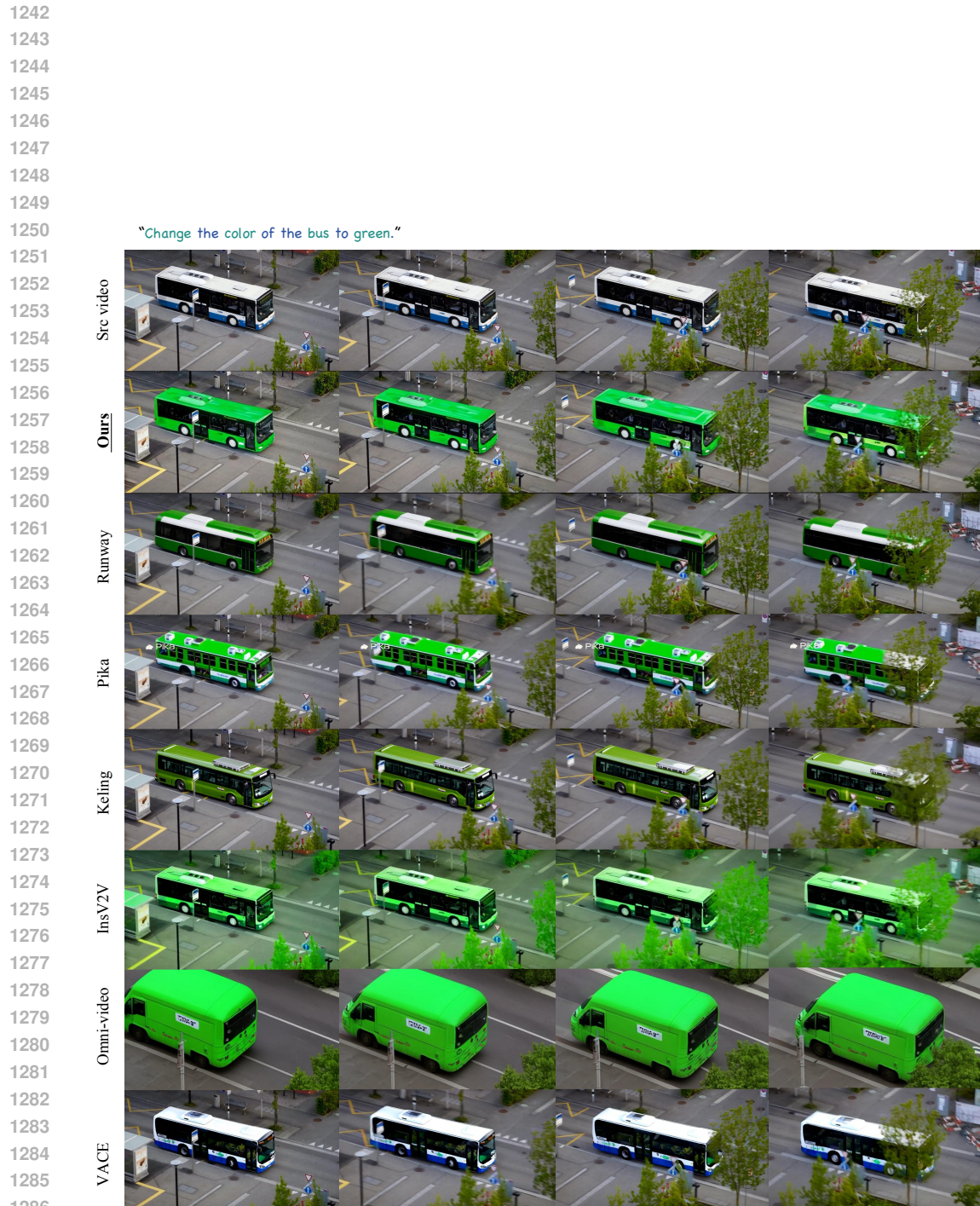


Figure 23: Visual comparsion on VIE-Bench.



Figure 24: Visual comparsion on VIE-Bench.

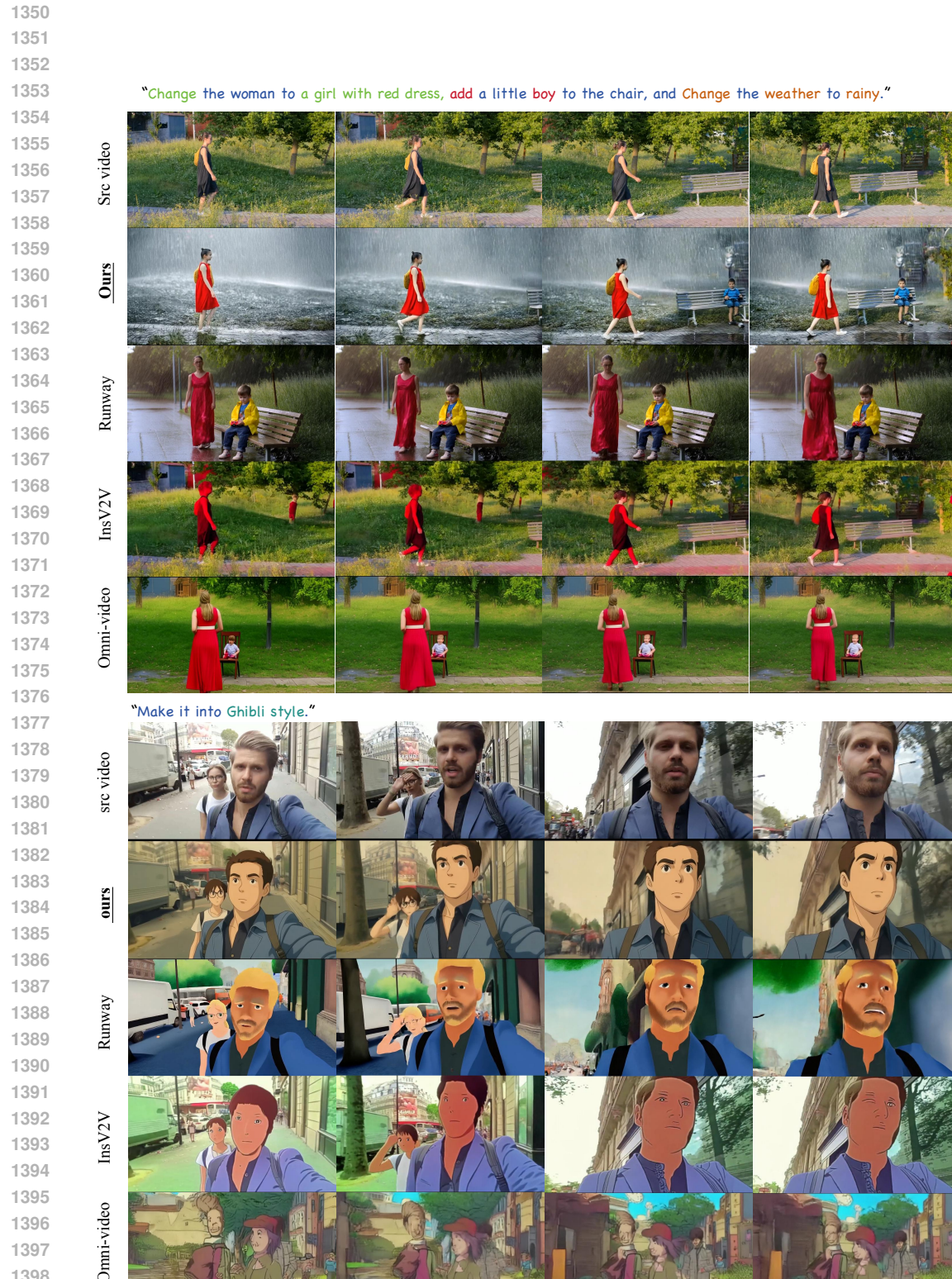


Figure 25: Visual comparsion on VIE-Bench.

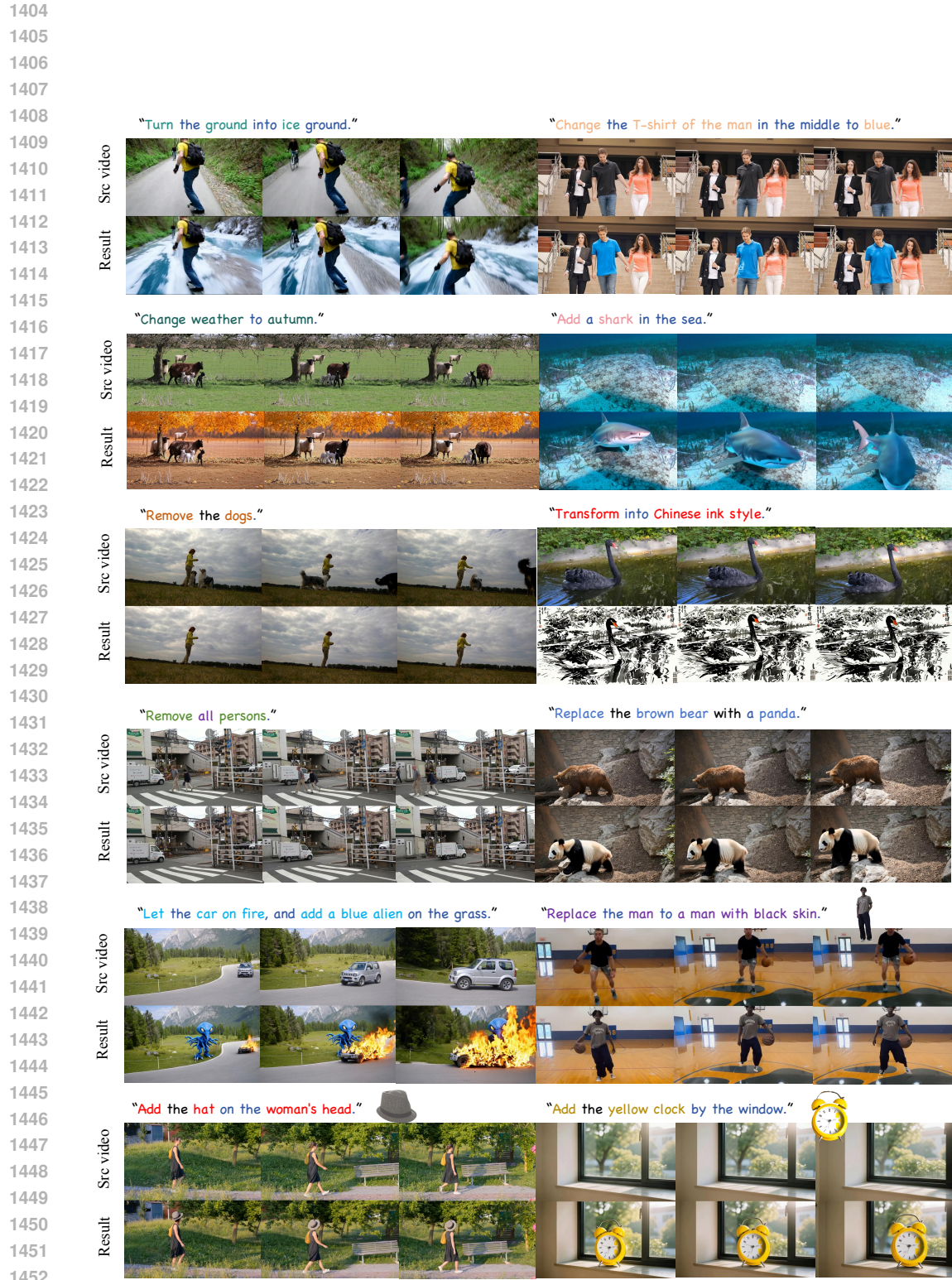


Figure 26: More video editing results of our method.

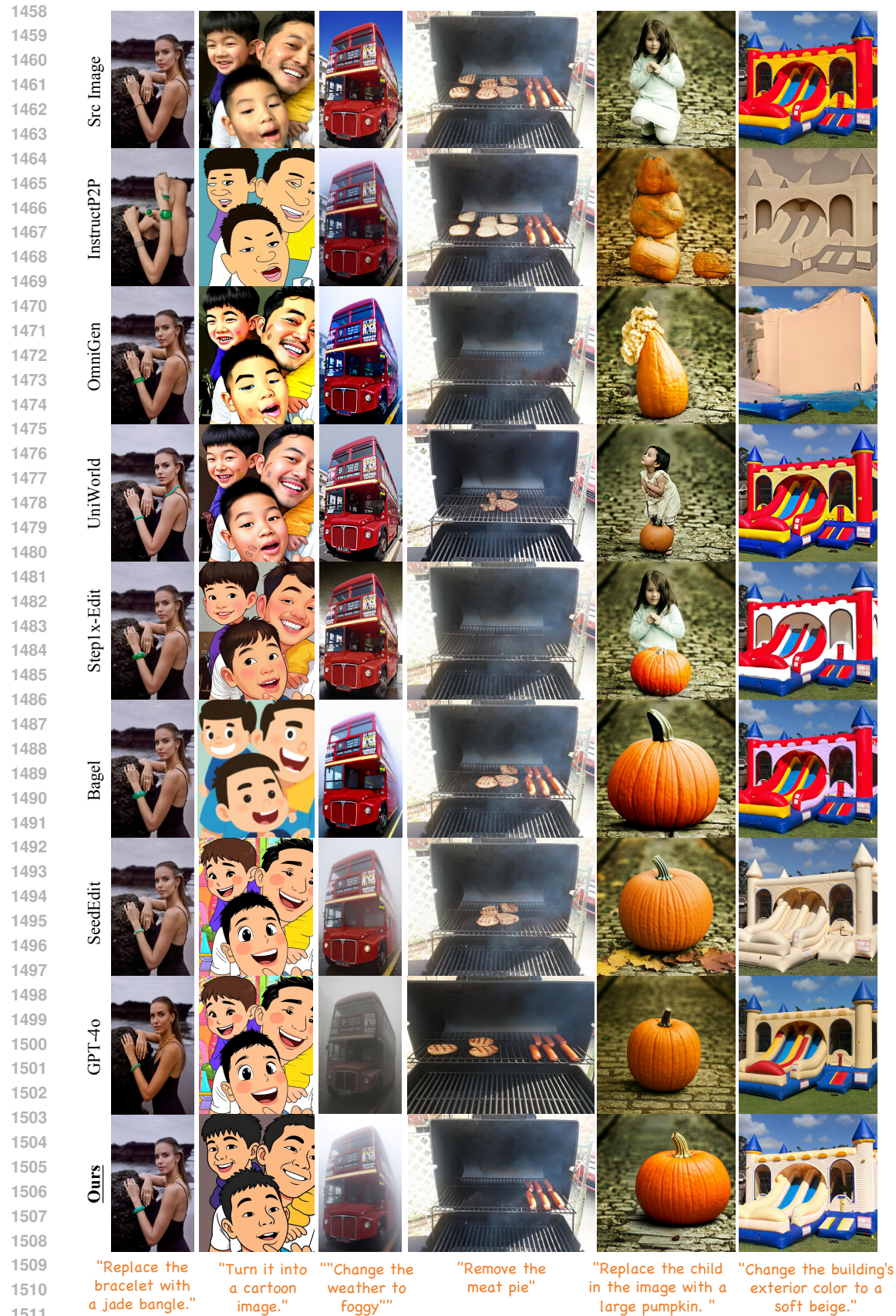


Figure 27: Visual comparsion on image editing.